Electrostatic Interactions in Wild-Type and Mutant Recombinant Human Myoglobins†

Raghavan Varadarajan,‡ David G. Lambright, and Steven G. Boxer*

Department of Chemistry, Stanford University, Stanford, California 94305

Received September 29, 1988; Revised Manuscript Received November 30, 1988

ABSTRACT: Residue Val68 in human myoglobin has been replaced by Asn, Asp, and Glu with site-directed mutagenesis. Purified proteins were characterized by isoelectric focusing and by absorption, CD, and NMR spectroscopy. These studies demonstrated that Mb is able to tolerate substitution of the buried hydrophobic residue Val68 by Asn, Asp, and Glu. In the metaquo derivatives of the Glu and Asp mutants, the negative charge at residue 68 is stabilized by a favorable Coulombic interaction with the heme iron. In the absence of this interaction, as in the metcyano and ferrous deoxy derivatives, the relatively nonpolar protein interior cannot stabilize an isolated buried negative charge, and the carboxylate is either protonated or stabilized via a salt bridge with the nearby distal histidine. Hence in the Asp and Glu mutant proteins, both reduction and cyanide binding are accompanied by proton uptake by the protein. The apoproteins were prepared and reconstituted with the chlorophyll derivative zinc pyrochlorophyllide *a*. Absorption and fluorescence spectra were quite similar for wild-type and all mutant proteins reconstituted with this derivative. These results do not support the point charge model for the red shifts observed in the spectra of chlorophylls associated with photosynthetic proteins. From the pH dependence of the absorption spectrum of zinc pyrochlorophyllide *a* in the Glu mutant, the apparent pK_a of the buried glutamate residue was estimated to be 8.9. This increase of 4.4 pH units, over the value for Glu in aqueous solution, provides a measure of the polarity of the protein interior.

Electrostatic interactions are important in determining the structure, stability, and dynamics of a folded protein. Despite their obvious importance, the calculation of electrostatic interaction energies in proteins is complicated by the very large number of interacting groups. It is therefore important to make experimental measurements of such interactions in order to test and improve the accuracy of the various theoretical methods currently available (Gilson & Honig, 1988; Warshel & Russell, 1985; Warwicker & Watson, 1982). Most previous experimental measurements of the energetics of charge–charge interactions have concentrated on charged residues that are accessible to aqueous solvent (Russell & Fersht, 1987; Rees, 1980). The solvation of these charged groups by aqueous solvent results in a high measured value of the effective dielectric constant. In order to obtain information about the polarity and dielectric properties of a protein interior, it is necessary to measure interaction energies between buried charged residues (Gilson et al., 1985; Moore et al., 1986).

Our original motivation for this work was the suggestion by Honig and co-workers that buried point charges may have a very significant effect on the spectral properties of chromophores bound in the interior of proteins, notably retinal in bacteriorhodopsin (Honig et al., 1976) and chlorophylls and bacteriochlorophylls in photosynthetic proteins (Eccles & Honig, 1983). Since we had demonstrated earlier that chlorophylls and bacteriochlorophylls can be substituted for heme in the heme binding pocket of sperm whale Mb[1] (Wright & Boxer, 1981; Lambright et al., unpublished results), it was natural to use site-directed mutagenesis to create potentially charged mutants of this synthetic chromophore–protein complex as a test case for the point charge model. As described below, the very large spectral shifts predicted by the model are not observed for these particular mutants; nonetheless, small spectral shifts are observed and can be used as an indicator of the protonation state of nearby amino acid side chains. Furthermore, complexes with zinc(II) pyrochlorophyllide *a*[2] (ZnPChl*a*) and zinc(II) protoporphyrin IX (ZnPPIX) prove to be very useful models for the five-coor-

Table I: Nomenclature Used To Describe Wild-Type (WT) and Mutant Human Mb's

myoglobin	mutation(s)	expression vector
WTMb		pMb3
C110A	Cys110 → Ala	pMbC110A
V68D	Val68 → Asp	pMbV68D
V68E	Val68 → Glu	pMbV68E
V68D′	Val68 → Asp, Cys110 → Ala	pMbV68D′
V68E′	Val68 → Glu, Cys110 → Ala	pMbV68E′
V68N′	Val68 → Asn, Cys110 → Ala	pMbV68N′

† This work was supported in part by NIH Grant GM 27738. S.G.B. is the recipient of a Presidential Young Investigator Award (matching funds from the Monsanto Corp.). The 500-MHz NMR spectrometer was funded by grants from the National Science Foundation (DMB-8515942) and from the National Institutes of Health (1-51-RR-2733-01).

‡ Present address: Department of Molecular Biophysics and Biochemistry, Yale University, New Haven, CT 06511.

[1] Abbreviations: Mb, myoglobin; ZnPChl*a*, zinc pyrochlorophyllide *a*; ZnPPIX, zinc protoporphyrin IX; Hb, hemoglobin; kb, kilo base pair(s); Tris·HCl, tris(hydroxymethyl)aminomethane hydrochloride; EDTA, ethylenediaminetetraacetic acid; DTT, dithiothreitol; SDS, sodium dodecyl sulfate; PAGE, polyacrylamide gel electrophoresis; MOPS, 3-(*N*-morpholino)propanesulfonic acid; TEMED, *N,N,N′,N′*-tetramethylethylenediamine; SW, sperm whale; ppm, parts per million; NOESY, nuclear Overhauser effect spectroscopy; COSY, correlation spectroscopy; UV–vis, ultraviolet–visible; $E^{o\prime}$, standard reduction potential; [^{2}H]TSP, [$^2H_4$](trimethylsilyl)propionic acid.

[2] A chlorophyll *a* derivative in which the phytyl side chain has been cleaved, the carbomethoxy group at position 10 has been replaced by a hydrogen, and Mg has been replaced with Zn. This latter replacement enhances the chemical stability of the chlorin.

0006-2960/89/0428-3771$01.50/0 © 1989 American Chemical Society

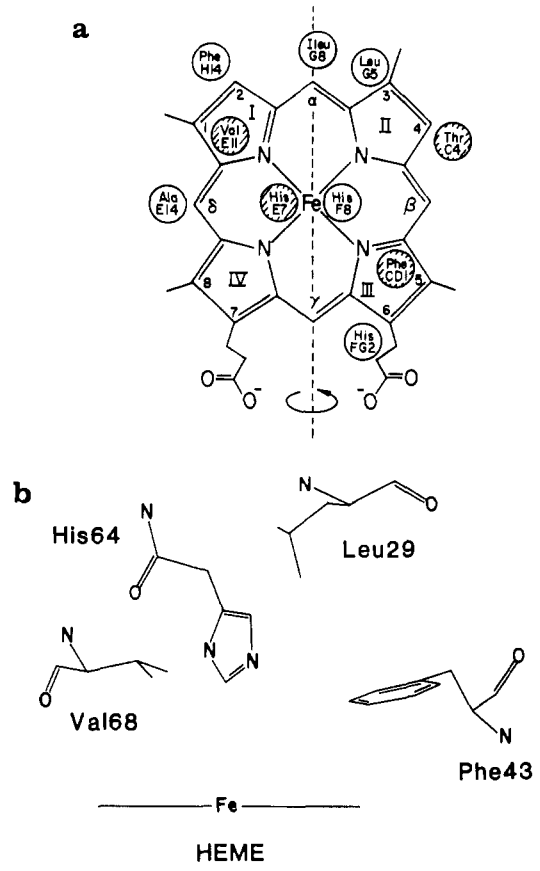

FIGURE 1: (a) Heme apoprotein contacts in the pocket of SWMb. Open circles indicate proximal residues and shaded circles distal ones. Heme vinyl groups at positions 2 and 4 are omitted for clarity. The dotted line indicates the approximate C_2 axis of symmetry of the heme [adapted from La Mar et al. (1978)]. (b) Positions of distal amino acids relative to the heme ring in metaquoSWMb (Takano, 1977) are shown in projection onto a plane approximately perpendicular to the plane of the four heme nitrogens.

dinate, neutral deoxy state of the less stable Mb mutants.

We have previously reported the isolation of a cDNA clone for human Mb as well as an efficient method for overproduction of the protein in *Escherichia coli*. Although an X-ray structure for human Mb is not yet available, the residues in the heme pocket as well as its optical, ligand binding, NMR, and redox properties are nearly identical with those of sperm whale Mb (SWMb) (Varadarajan et al., 1985, 1989). Residue Val68 (also denoted ValE11) is situated below heme ring 1 on the distal side of the heme pocket and within van der Waals contact of the heme (Figure 1). In the X-ray structure of sperm whale metaquoMb (Takano, 1977; Lee & Richards; 1971) this residue is completely inaccessible to external solvent. Interactions of charged groups at this position with the porphyrin would therefore be mediated principally by the protein, rather than by external solvent. In the naturally occurring, single-site hemoglobin (Hb) mutants Hb Milwaukee and Hb Bristol, Val68 is replaced in the β-chains by Glu and Asp, respectively (Perutz et al., 1972; Steadman et al., 1970). The fact that Hb is able to tolerate such drastic changes at this residue position prompted us to replace Val68 with Glu and Asp in human Mb. In order to determine whether the Asp was protonated when buried in the protein, we also replaced Val68 with Asn since a protonated Asp is structurally very similar to Asn. A description of the amino acid substitutions present in each of the mutant proteins can be found in Table I. Purified mutant proteins were characterized by isoelectric focusing, absorption, CD, and NMR spectroscopy. Cyanide binding constants were measured in order to obtain estimates of the electrostatic interaction between potentially charged substituents at residue 68 and the heme iron. The large changes in the redox thermodynamics of the heme iron observed in these mutant proteins have been reported separately (Varadarajan et al., 1989).

Materials and Methods

Site-Directed Mutagenesis. Unless otherwise specified, all enzymes used were from New England Biolabs. All DNA manipulations were as described in Messing (1983). Site-directed mutagenesis was performed in M13mp11FXMb and its derivatives (Varadarajan et al., 1985) essentially as described by Kunkel (1985). The dut$^-$, ung$^-$ *E. coli* strain RZ1032 used was obtained from T. Kunkel. Probable mutants were sequenced by dideoxy sequencing (Sanger, 1981) to ensure that no additional mutations in the Mb coding sequence had occurred. The *Bam*HI–*Hin*dIII fragment containing the mutant Mb coding region was then ligated to the *Bam*HI–*Hin*dIII fragment from pMb3 to give the desired expression vector (Table I).

Cysteine Codon Replacement. pMbV68N and pMbC110A (0.5 μg each) were digested with 5 units of *Afl*II (Amersham) for 2 h at 37 °C. Five units of *Hin*dIII was added and digestion continued for 1 h. The approximately 3 kilo base pair (kb) fragment from pMbV68N was ligated to the 505 base pair fragment from pMbC110A to give pMbV68N′. This was transformed into strain AR68 (obtained from A. Shatzman) according to the procedure described for transformation into strain MZ1 (Varadarajan et al., 1985). Several transformants were picked and induced. A control transformation using only the 3-kb fragment gave no transformants. pMbV68E′ and pMbV68D′ were prepared in a similar fashion.

Protein Purification. AR68 cells containing the appropriate expression vector were grown at 28 °C in L Broth containing 50 μg/mL ampicillin in a 200-L fermentor to an optical density (595 nm) of 1.0. The cells were induced by raising the temperature to 42 °C. Growth was continued at this temperature for 2 h; the cells were harvested and stored at −20 °C. The cells were lysed and the inclusion bodies resolubilized in 50 mM Tris·HCl, pH 9.0, 100 mM NaCl, 1 mM EDTA, 8 M urea, and 1 mM DTT, essentially as described by Marston et al. (1984). The solution was then centrifuged at 10 °C, 12000*g*, for at least 1 h and the supernatant dialyzed at 4 °C against 10 volumes of 50 mM Tris·HCl, pH 9.0, and 1 mM EDTA. For proteins containing Cys110, the dialysis buffer also contained 1 mM DTT. The protein was then dialyzed for 10–12 h (two buffer changes) against 10 volumes of 10 mM Tris·HCl, pH 9.0, and 1 mM EDTA. Dialysis at pHs lower than 9.0 results in protein precipitation. The dialyzate was then centrifuged at 4 °C, 12000*g*, for 30 min. The fusion protein concentration was normally about 1–2 mg/mL as estimated by SDS–PAGE (Laemmli, 1970). To the supernatant at 4 °C was added 1–2 equiv of a 10 mg/mL solution of heme in 0.2 N NaOH. Addition of larger amounts of heme does not increase the yield of reconstituted protein and complicates further purification. After 15 min at 4 °C the reconstituted fusion protein was incubated at 16 °C for 15 min and then digested with 50 μg/mL trypsin (type III, Sigma) at 16 °C. After 2 h, the pH of the solution was raised to 9.2 and the protein loaded onto a 5 × 10 cm DE-52 column (Whatman) that had been equilibrated with 5 mM Tris·HCl, pH 9.0, at 4 °C. At this stage the fusion protein has been digested to an intermediate product of molecular weight approximately 18 000 that probably results from tryptic cleavage of the fusion protein at a Lys ten amino acids upstream from the end of the FX_a site (Nagai & Thogersen, 1984). This

cleavage product was eluted with 50 mM Tris·HCl, pH 7.7, and concentrated with an Amicon YM10 membrane. Trypsin was added to a final concentration of 50 μg/mL and the intermediate digested overnight at 16 °C to give the desired product. The protein was dialyzed for 2 h at 4 °C against 5 mM Tris·HCl, pH 9.0, loaded onto a DE-52 column, eluted with 40 mM Tris·HCl, pH 9.0, concentrated to about 2 mg/mL, and precipitated by saturating the solution with ammonium sulfate.

Apoprotein Preparation. Unless otherwise stated, all apoprotein preparations and reconstitutions were performed with the protein at 4 °C in order to minimize aggregation. A total of 5 mg of protein in 40 mM Tris·HCl, pH 9.0, was dialyzed twice against deionized H_2O. The pH of the protein solution was reduced to 2.4 with 0.25 N HCl and the heme extracted twice with methyl ethyl ketone (Teale, 1959). The apoprotein was dialyzed three times against 1 mM HCl (pH 3.0). For proteins that contained Cys110, all dialysis buffers were saturated with Ar. In addition, after heme extraction, the dialysis buffer also contained 1 mM DTT.

Reconstitution with ZnPPIX. A total of 1–2 equiv of a freshly prepared 5 mg/mL solution of the porphyrin in 1 N NaOH was added to the apoprotein in 50 mM Tris·HCl, pH 8.0. After 15 min, the reconstituted protein was dialyzed against 5 mM Tris·HCl, pH 8.9, and purified on a DE-52 column. Alternatively, the reconstitutions were carried out on the unpurified apofusion proteins. Tryptic digestion at 16 °C and protein purification were then carried out as described above.

Reconstitution with ZnPChla. ZnPChl*a* was prepared as described by Bucks (1981). A total of 8 mg of ZnPChl*a* was dissolved in 0.5 mL of dimethyl sulfoxide. The solution was diluted with 0.5 mL of 10 mM sodium phosphate, pH 6.3, and loaded onto a 10 × 1.5 cm S-200 column (Pharmacia) equilibrated with 10 mM sodium phosphate, pH 6.3. ZnPChl*a* precipitated onto the column, coloring the top 2 cm dark green. Each such column was used for several separate reconstitutions of wild-type and mutant apoproteins. Apoprotein solution (pH 3.0) was loaded onto the column at a flow rate of 0.2 mL/min; 10 mM sodium phosphate, pH 6.3, was then passed through the column at 0.2 mL/min for about 1 h, at which point a green band eluted. This was concentrated to approximately 0.5 mL with Centricons and further purified by passage through a 1 × 15 cm S-200 column.

Isoelectric Focusing. Isoelectric focusing was carried out on thin-layer, polyacrylamide gel plate apparatus from either Hoefer or LKB. Precast gels (LKB) were used which had a pH range of 3.5–9.5. Small (10–20 μg) quantities of Mb were detected by Coomassie blue staining. Larger quantities were visible to the naked eye. pH along the gel was determined by measuring the positions of protein standards (Pharmacia) having known isoelectric points.

Nondenaturing PAGE. Gels contained 5% acrylamide, 0.125% bis(acrylamide), 0.05% ammonium persulfate, 0.11% TEMED, and 60 mM MOPS, pH 7.0–7.7 (McClellan, 1984). The anodic and cathodic buffers were the same as the buffer in the gel. Samples were run from cathode to anode at 150 V for 2 h in a minigel apparatus from Hoefer. An anaerobic polyacrylamide gel was poured and run in an anaerobic box. The gel contained 5% acrylamide, 0.125% bis(acrylamide), 0.005% ammonium persulfate, and 60 mM MOPS, pH 7.0. Protein samples were deoxygenated by overnight dialysis against Ar-saturated buffer. Where necessary, proteins were reduced with sodium dithionite just prior to loading. Electrophoresis was carried out at 150 V for 1.5 h.

NMR Spectroscopy. A total of 40 mg of protein in the form of an ammonium sulfate precipitate was dialyzed at 4 °C, once against 50 mM Tris·HCl, pH 9.0, and three times against deionized water. The protein was exchanged three to four times with D_2O and concentrated to approximately 200 μL with a Centricon. The sample was diluted into 5 mL of CO-saturated, deuterated 10 mM sodium phosphate, pH 7.0 (uncorrected for the isotope effect), contained in a 5-mL Amicon concentrator with a YM10 Amicon membrane. Sodium dithionite was added to a final concentration of 10 mM, and the sample was concentrated under 20 psi CO to a final protein concentration of 2–4 mM. The sample was transferred to an NMR tube under a stream of CO and the NMR tube capped and sealed with Parafilm. All NMR experiments were conducted at 16 °C and 500 MHz on a GE GN500 spectrometer with a 16-bit ADC. Phase-sensitive ^1H NOESY spectra were acquired with a 250-ms mixing time according to the method suggested by States et al. (1982). COSY and double quantum filtered COSY data were acquired by standard methods (Marion & Wüthrich, 1983; Rance et al., 1983).

pK_a Measurement. The pK_a of the heme-bound water molecule in metaquoMb and metaquoV68N′ was measured by a spectrophotometric titration of the protein (George & Hanania, 1952). The buffer used was 10 mM sodium phosphate, 10 mM sodium borate, and 100 mM NaCl. The pH of the protein solution was increased by adding aliquots of 1–5 N NaOH. The pH of the protein solution after each addition of NaOH was measured in the cuvette with an Orion pH meter equipped with an Ingold combination electrode. The apparent pK_a of the pH-dependent spectral shift of ZnPChl*a*–V68E′ was measured by a similar procedure. The buffer used was 10 mM sodium phosphate and 10 mM sodium borate.

Cyanide Binding Constant Determination. The 2 M and 100 mM KCN stock solutions were prepared fresh before the start of each titration. The purity of the KCN used was checked by performing a Leibig titration (Kolthoff et al., 1969). Where necessary, the pH of the KCN stock solutions was adjusted to the desired value with concentrated HCl in a hood. Since cyanide binding leads to characteristic changes in the visible absorption spectrum of the protein, the binding constant was measured by monitoring the absorbance at 409 nm as a function of added cyanide concentration.

The apparent dissociation constant (K_{da}) for cyanide is given by

$$K_{da} = [Mb][CN]/[MbCN] \quad (1)$$

[Mb] is the concentration of protein without cyanide bound. For C110A and V68N′ this consists of a mixture of metaquo and methydroxy derivatives; for V68E′ and V68D this consists solely of the metaquo derivative. [MbCN] is the concentration of the metcyano derivative and [CN] is the concentration of free cyanide. [CN] includes both cyanide anions and HCN. Equation 1 can be rewritten in the form

$$A = (A_1K_{da} + A_2[CN])/([CN] + K_{da}) \quad (2)$$

where A is the sample absorbance at a total cyanide concentration $[CN]_t$, A_1 is the sample absorbance before any cyanide has been added, and A_2 is the sample absorbance when all protein present is in the metcyano form. For V68D and V68E′, which have large dissociation constants, [CN] is well approximated by $[CN]_t$. Since it was not possible to experimentally determine A_2 for V68D and V68E′, both A_2 and K_{da} were determined with a nonlinear least-squares fit of the data to eq 2 (Press et al., 1987). For C110A and V68N′ it is no longer valid to approximate [CN] by $[CN]_t$. If the total

Table II: Isoelectric Points of Derivatives of Wild-Type and Mutant Myoglobins (See Figure 2)[a]

derivative	myoglobin				
	WTMb	C110A	V68D′	V68E′	V68N′
metaquo	7.20	7.27	6.64	6.63	7.14
ZnPPIX		6.76	6.76	6.76	6.76
ZnPChl*a*		7.31	7.31	7.31	7.31
CO	6.62	6.65			

[a] The estimated error is ±0.03 on the basis of two to three separate determinations of each isoelectric point.

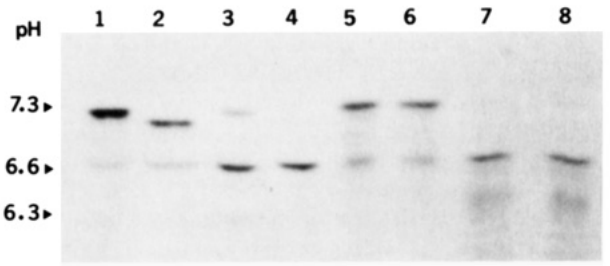

FIGURE 2: Isoelectric focusing gel: (lane 1) metaquoC110A; (lane 2) metaquoV68N′; (lane 3) metaquoV68E′; (lane 4) metaquoV68D′; (lane 5) ZnPChl*a*–C110A; (lane 6) ZnPChl*a*–V68E′; (lane 7) ZnPPIX–C110A; (lane 8) ZnPPIX–V68E′. The fainter bands of lower isoelectric point in each lane arise from reduced protein which is formed in the gel and/or traces of deamidated protein.

concentration of protein present is $[Mb]_t$, then at a total cyanide concentration $[CN]_t$ it can be shown that

$$[CN] = [CN]_t - [MbCN] = [CN]_t - \{[Mb]_t(A_1 - A)/(A_1 - A_2)\} \quad (3)$$

where A_2 can be obtained experimentally in this case. K_{da} is then determined as described above.

Results and Discussion

Cysteine Codon Replacement. Wild-type human Mb (WTMb) contains a single Cys at position 110. Since this causes problems in protein purification and apoprotein preparation, the Cys was replaced by Ala with site-directed mutagenesis to give the mutant protein C110A. This change has no effect on the electronic absorption spectra, 1D NMR spectra (of the CO derivatives), or on redox and cyanide binding properties of the protein, although there is a small increase in the isoelectric point (Table II). The Cys codons in the expression vectors pMbV68D, pMbV68E, and pMbV68N were replaced by an Ala (the residue at this position in most other mammalian Mb's) by means of a simple cloning procedure. The new proteins, which were double mutants at positions 68 and 110, were named V68D′, V68E′, and V68N′ and are spectroscopically and functionally indistinguishable from V68D, V68E, and V68N, respectively.

Isoelectric Focusing. The metaquo derivatives of V68E′ and V68D′ have a p*I* that is about 0.5 pH unit lower than those of the metaquo derivatives of wild type and V68N′ (Table II, Figure 2) and similar to the p*I* of reduced (ferrous) Mb, suggesting that in metaquoV68D′ and metaquoV68E′ the carboxylate side chains of Asp and Glu are ionized at the pH of the isoelectric point (pH 6.65), despite being buried inside the protein. The term metaquo refers to heme iron in the ferric oxidation state with water as the only possible exogenous ligand. It was not possible to determine the isoelectric points of either the deoxy or CO forms of V68D′ and V68E′ because these ferrous derivatives were readily oxidized by atmospheric O_2 back to the ferric form. Mb reconstituted with ZnPPIX (ZnPPIX–Mb) has been used as a model for the reduced deoxy state. Wild-type and all mutant proteins reconstituted with ZnPPIX were found to have approximately the same p*I* as oxyWTMb, metaquoV68D′, and metaquoV68E′. This suggests that the side chain of either the carboxylate at residue 68 or a nearby residue, most probably the distal histidine (Figure 1), is protonated in ZnPPIX–V68D′ and ZnPPIX–V68E′ at the p*I* (pH 6.76). It also suggests that either one of these residues is protonated in the deoxy and CO derivatives of V68E′ and V68D′.

Table III: Positions of Peak Maxima (λ_{max}, in nm) and Corresponding Millimolar Extinction Coefficients (ϵ) in the Absorption Spectra of the Metaquo Derivatives of Wild-Type and Mutant Myoglobins[a]

myoglobin	λ_{max} [(ϵ)]		
WTMb	409 (160)	500 (8.68)	632 (3.33)
V68D	409 (154)	500 (8.48)	622 (4.33)
V68E	408 (154)	500 (8.62)	620 (6.27)
V68N′	409 (138)	500 (8.49)	628 (3.88)

[a] The errors in ϵ, based on two to three separate determinations, are approximately ±5% of the listed value.

Nondenaturing PAGE. The electrophoretic mobilities of wild-type and mutant proteins were examined with nondenaturing polyacrylamide gels at pH's between 7.0 and 7.7. Under these conditions the metaquo derivatives of V68D′ and V68E′ had the same mobility as CO–C110A and higher mobilities than metaquoC110A and metaquoV68N′, consistent with the carboxylate side chains being charged in the metaquo forms of V68D′ and V68E′. In order to examine the mobilities of these two proteins in the reduced state, a gel was poured and run in an anaerobic box. The mobilities of V68D′ and V68E′ were unchanged upon reduction, confirming the assertion that reduction of the heme iron in V68E′ and V68D′ is accompanied by uptake of a proton.

Electronic Absorption Spectra. The heme iron binds a variety of ligands in both ferric and ferrous oxidation states. Spectra of the metcyano, deoxy, and CO derivatives of all mutant proteins are very similar to the corresponding wild-type derivatives with shifts in peak maxima being 2 nm or less. Extinction coefficients and peak maxima of wild-type and mutant metaquo derivatives are listed in Table III. Extinction coefficients were measured as described in Antonini and Brunori (1971). It is only in the metaquo form of the protein that the spectra of V68E and V68D differ noticeably from those of the other proteins (Figure 3). The peaks at 635 and 1025 nm in the absorption spectrum of the wild-type protein [assigned as ligand-to-metal charge-transfer bands (Makinen & Churg, 1983)] are shifted to 622 and 950 nm in metaquoV68D and to 620 and 900 nm in metaquoV68E. The spectrum of metaquoV68N′ is very similar to that of the wild-type protein. Since the interactions of a protonated Asp group with the heme should be very similar to those of an Asn, this is additional evidence that the carboxylate side chain in metaquoV68D is ionized even when buried in the protein.

The observed spectral shifts in metaquoV68D and metaquoV68E could be due to either global conformational changes in these proteins, localized changes in the ligands bonded at the heme iron, or the purely electrostatic effects of introducing a negative charge close to the heme iron. The lack of differences in other regions of the UV–vis and CD spectra (Varadarajan, 1988), as well as the resistance of both wild-type and mutant metaquo forms of the protein to tryptic digestion, makes it unlikely that there are large global conformational changes occurring in any of the mutant proteins. By analogy with Hb Milwaukee, in which the glutamate replaces the water molecule that is coordinated to the ferric heme iron in the

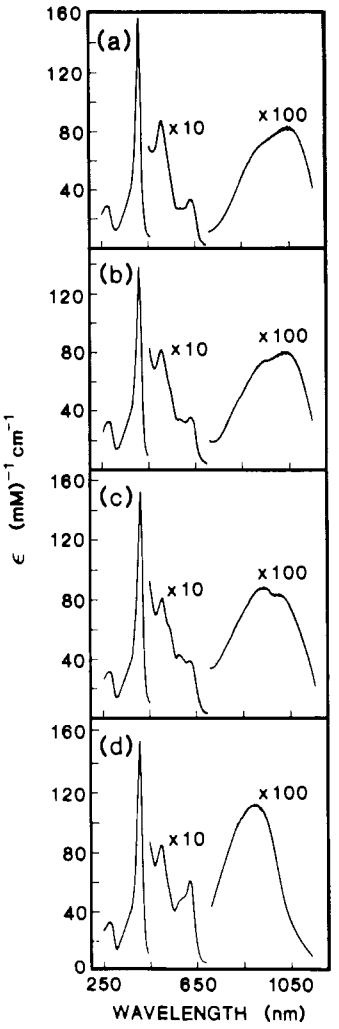

FIGURE 3: Absorption spectra of metaquo derivatives of (a) WTMb, (b) V68N′, (c) V68D, and (d) V68E, in 10 mM sodium phosphate, pH 6.0, at 28 °C.

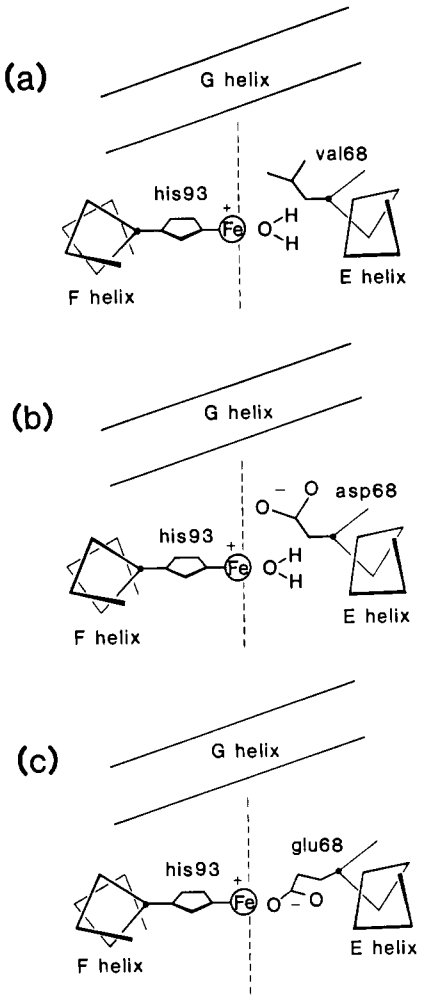

FIGURE 4: Proposed coordination of the heme iron in the metaquo derivatives of (a) WTMb, (b) V68D, and (c) V68E [adapted from Dickerson and Geiss (1983)].

wild-type protein (Perutz et al., 1972), it is very likely that the same is true for metaquoV68E. Examination of computer graphics models shows that the shortening of the side chain by one methylene group that occurs on going from Glu to Asp would make it impossible for the Asp carboxyl group to coordinate to iron without substantial global protein conformational changes. This implies that the observed spectral shifts in metaquoV68D are due to electrostatic effects, and as in the wild-type protein, water is the sixth ligand at the ferric heme iron. As expected, the ligand-to-metal charge-transfer bands are highly sensitive to electrostatic effects,[3] while the porphyrin ring centered $\pi\pi^*$ transitions are unchanged. The proposed coordination of the heme iron in the metaquo derivatives of WTMb, V68D, and V68E (Figure 4) is also consistent with results of NMR dispersion studies of these proteins (Zewert et al., personal communication).

One of the hydrogens of the heme-bound water molecule in metaquoMb is thought to be hydrogen bonded to the N3 nitrogen of the distal His (Antonini & Brunori, 1971). Deprotonation of the heme-bound water molecule in the metaquo derivatives of C110A and V68N′ to give the methydroxy form is accompanied by characteristic changes in the visible absorption spectra of these molecules. The pK_a of this water molecule was determined to be 8.8 and 8.1 in C110A and V68N′, respectively (Figure 5). This change in pK_a is in-

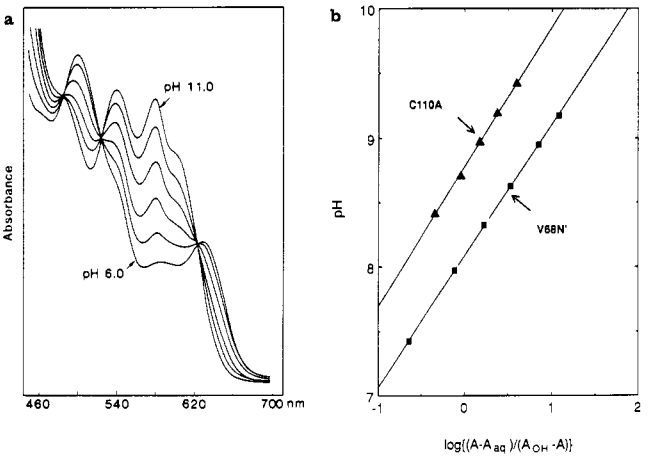

FIGURE 5: (a) Spectral changes accompanying deprotonation of the heme-bound water molecule in metaquoV68N′. (b) Determination of the pK_a at 28 °C in 10 mM sodium phosphate, 10 mM sodium borate, and 100 mM NaCl of the heme-bound water molecules in the metaquo derivatives of C110A and V68N′. A_{aq} and A_{OH} are the sample absorbances at pHs of 6.0 and 11.0 and correspond to the absorbances of the metaquo and methydroxy derivatives, respectively. A is the sample absorbance at intermediate pHs. Absorbance changes were monitored at 590 nm as a function of pH. The pK_a was determined from the intercept of a plot of log $\{(A - A_{aq})/(A_{OH} - A)\}$ vs pH.

[3] The stabilization of the ferric heme iron, due to a favorable electrostatic interaction with the negatively charged carboxylate at residue 68, results in an increase in the energies of ligand-to-metal charge-transfer transitions.

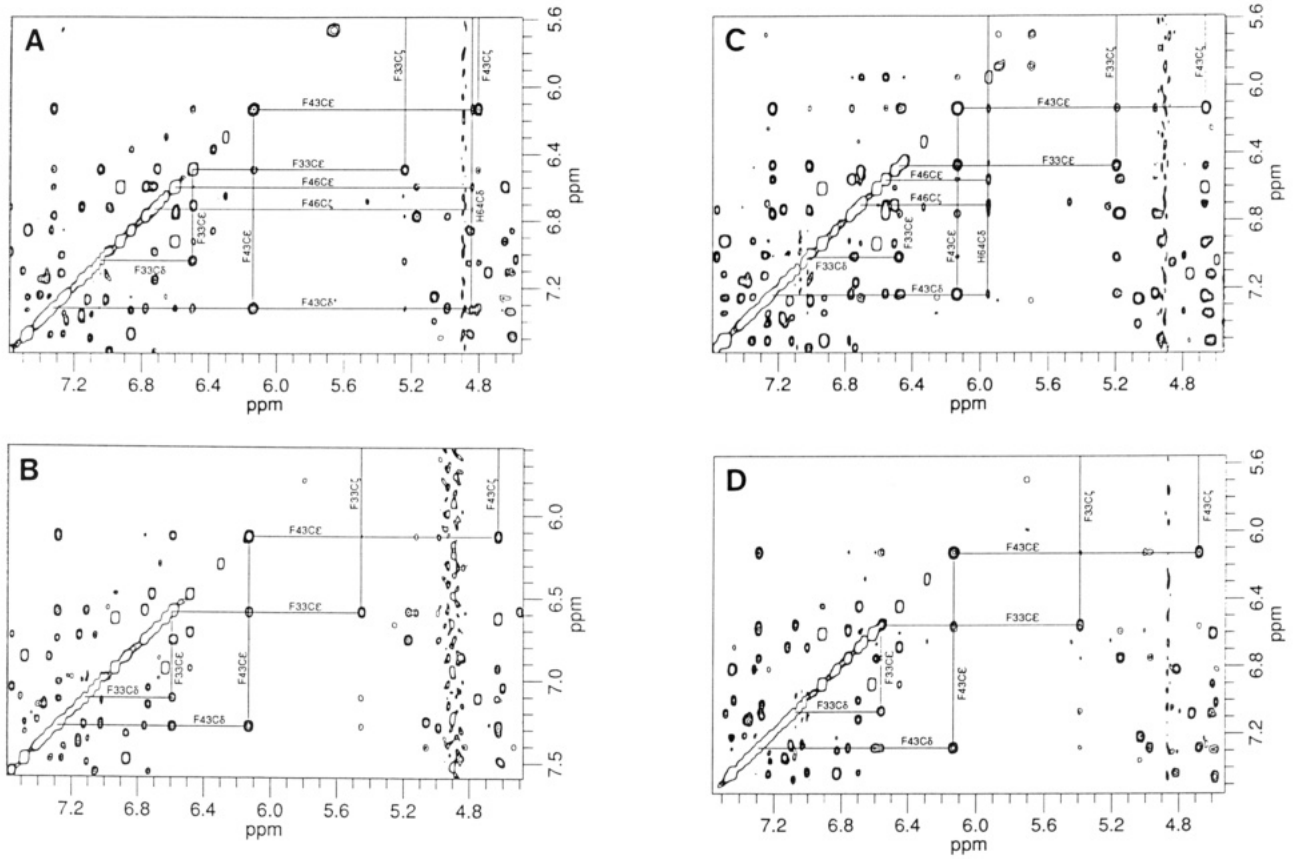

FIGURE 6: Regions of the 500-MHz phase-sensitive ^{1}H NOESY spectra containing intraresidue cross-peaks of ring protons of Phe43 in the CO derivatives of (A) C110A, (B) V68N′, (C) V68D, and (D) V68E′ in 50 mM sodium phosphate/D_2O, pH 7.0, 16 °C (250-ms mixing time).

dicative of an interaction involving the Asn, the heme-bound water, and possibly the distal His. By contrast, the absorption spectra of the metaquo derivatives of V68E and V68D are independent of pH in the pH ranges 5.0–11.0 and 5.5–10.5, respectively. Outside of these pH ranges protein denaturation occurs. Formation of the methydroxy form in these two proteins is apparently disfavored because of the electrostatic repulsion that would result between the carboxylate side chain at residue 68 and the heme-bound hydroxide anion. The pK_a's of Asp and Glu in aqueous solution are 4.0 and 4.5, respectively (Matthew, 1985). The pH independence of the absorption spectra of metaquoV68D and metaquoV68E also indicates that the pK_a's of the buried residues Asp68 and Glu68 in these two proteins are unlikely to be substantially greater than the pK_a's for Asp and Glu in aqueous solution, probably because the negatively charged carboxylates are stabilized by a Coulombic interaction with the positively charged heme iron.

NMR Spectroscopy. Sperm whale CO-Mb which contains a diamagnetic heme iron has been characterized extensively by a variety of 1D and 2D NMR techniques (Shulman et al., 1970; Dalvit & Wright, 1987), and several protons from each of the residues in van der Waals contact with the heme ring have been assigned. We have used 2D NMR spectroscopy of the CO derivatives to characterize the orientation of the heme ring relative to the heme pocket, as well as the nature and extent of structural differences between C110A and the other mutant proteins.

The heme ring in Mb's from several different species has been shown by X-ray crystallography to have the orientation shown in Figure 1a in which Val68 is situated above heme ring 1 (Takano, 1977; Scouloudi & Baker, 1978). However, NMR studies of Mb's reconstituted with a variety of hemes have demonstrated the presence of a minor orientation in solution in which the heme is rotated 180° about its pseudo C_2 axis of symmetry (Jue & LaMar, 1984). NMR studies of monomeric hemoglobins from *Glycera dibranchtia* (Cooke & Wright, 1985) and *Chironomus thummi thummi* (LaMar et al., 1978) demonstrate that this reversed orientation is the predominant one in solution for these two proteins. Since it has not yet been established which protein–chromophore interactions determine the heme orientation preferred in solution, it was important to determine this orientation for all myoglobins studied.

V68D and V68E have substantially lower redox potentials than C110A and V68N′ (Varadarajan et al., 1989). Consequently, the CO derivatives of these two proteins are less stable than CO-C110A and are much more susceptible to oxidation to the metaquo form. Sample oxidation was minimized by concentrating the CO derivatives in an Amicon under CO, transferring to the NMR tube under a stream of CO, and sealing the cap with a layer of Parafilm. In order to minimize protein unfolding and aggregation, experiments were carried out at 16 °C. The assignment of proton chemical shift was greatly facilitated by the fact that the residues in the heme pocket are highly conserved between C110A and SWMb. Hence very similar patterns of NOESY and COSY cross-peaks are observed in the CO derivatives of SWMb, C110A, and other mutant proteins. For example, the spin system of Phe43 exhibits a characteristic set of intraresidue cross-peaks in the NOESY/COSY spectra of CO-SWMb (Dalvit & Wright, 1987). A similar set of cross-peaks is found in the NOESY spectra (Figure 6) and COSY spectra (data not shown) of all the mutant Mb's leading to assignments of Phe43 ring protons in these proteins. Heme meso proton peaks occur well resolved from other peaks in the 9.0–10.5-ppm region of the spectrum. Three of the four heme meso protons are located

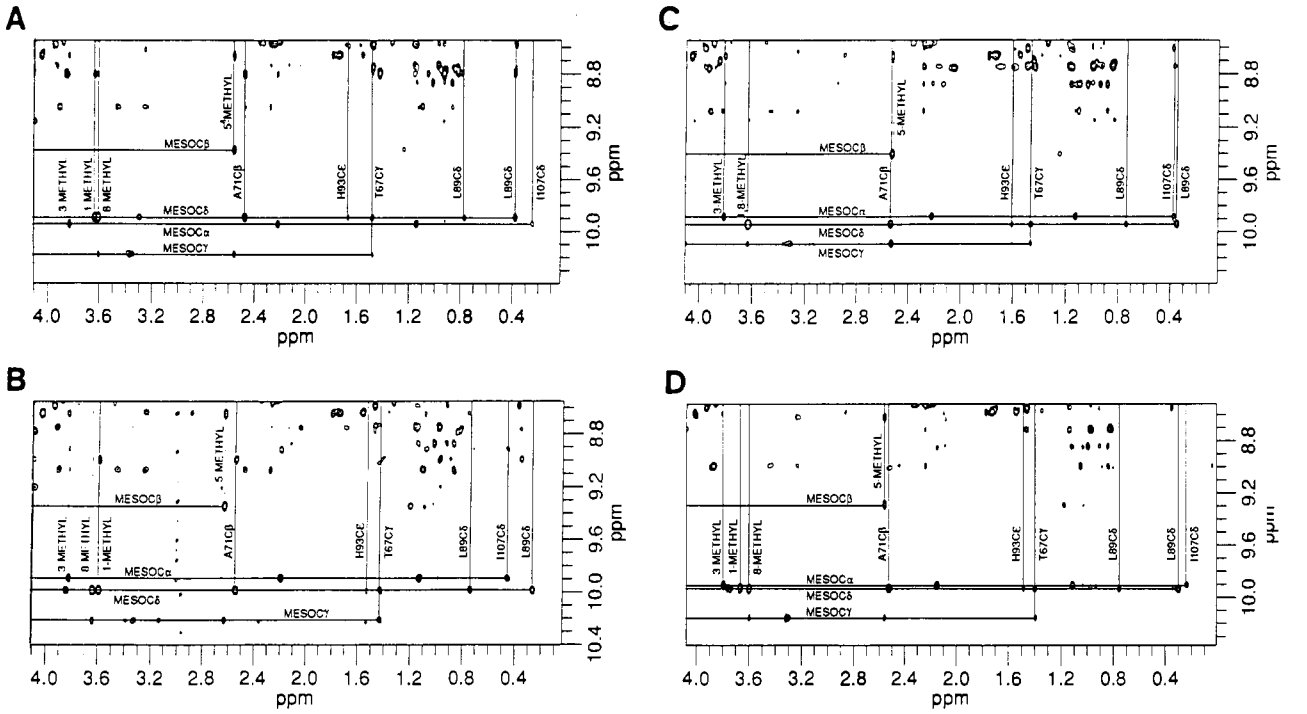

FIGURE 7: Regions of the 500-MHz phase-sensitive ^{1}H NOESY spectra containing cross-peaks between heme meso and heme methyl protons in the CO derivatives of (A) C110A, (B) V68N′, (C) V68D, and (D) V68E′ in 50 mM sodium phosphate/D_2O, pH 7.0, 16 °C (250-ms mixing time).

close to heme methyl (Me) groups (Figure 1a). It is therefore expected that the NOESY spectrum will contain strong cross-peaks between these meso protons and the corresponding Me groups which normally occur between 3 and 4 ppm. The δ-meso proton is easily identifiable in the NOESY spectrum of CO-C110A since it is the only meso proton that gives strong cross-peaks to two sets of heme methyl group protons (1-Me and 8-Me) at about 3.6 ppm (Figure 7). Assignment of the heme γ-meso proton was based on the fact that this is the only meso proton that cannot give any cross-peaks to heme Me protons (Figure 1a). One of the two remaining meso protons gives a strong cross-peak to a resonance at 2.54 ppm. This is consistent only with the assignment of these resonances to the β-meso and the 5-Me protons, respectively, and with the heme having the orientation shown in Figure 1a. The upfield shift of the 5-Me protons results from their proximity to Phe43. Consistent with these assignments is the presence of cross-peaks between the Phe43Cδ and the β-meso protons and between the Phe43Cδ and the 5-Me protons. An identical set of cross-peaks between heme meso, heme methyl, and Phe43 ring protons was observed in the NOESY spectrum of CO-SWMb (Dalvit & Wright, 1987). The same procedure was used to determine the orientation of the heme ring in the other mutant proteins. In all cases the orientation was found to be as shown in Figure 1a. With these assignments for heme and Phe43 protons as a starting point, NOESY and COSY connectivities were used to obtain a consistent set of assignments for residues in and around the heme pocket. Some of these assignments are listed in Table IV.

Protons close to the heme ring can experience large ring current shifts. The magnitude of these shifts is very sensitive to the position of the protons relative to the ring. Most protons belonging to residues in the heme pocket have nearly identical chemical shifts in different mutants, which provides very strong evidence that, in solution, there are no large conformational differences between any of the proteins studied. A striking exception to this are the Cε and Cδ protons of the distal His (His64) in CO-V68D. The His64Cε proton in CO-V68D is upfield shifted by approximately 1 ppm relative to its position in the other proteins. The His64Cδ proton in CO-V68D is downfield shifted 1.1 ppm relative to its position in CO-C110A. The His64Cδ proton has not been assigned in CO-V68E′ and CO-V68N′, possibly because it may have shifted slightly from its 4.84 ppm position in CO-C110A to a position underneath the residual HDO peak at 4.90 ppm.

In the crystal strcture of metaquoSWMb, the Nε nitrogen of His64 is situated at a distance of about 3 Å from the γMe groups of Val68 (Takano, 1977). In CO-SWMb, His64 has a pK_a of less than 5.0 because it is buried in the interior of the protein (Mabbutt & Wright, 1985). When Asp was substituted in place of Val68 by computer graphics, it could be placed in close proximity to His64 without major protein rearrangement. The large differences in chemical shift between the His64Cε protons in CO-V68D and CO-V68N′

Table IV: Chemical Shifts (in ppm Relative to [^{2}H]TSP) for Selected Protons Close to the Heme Group (with the Exception of Met131Cε) in the CO Derivatives of C110A, V68N′, V68D, and V68E′[a]

	myoglobin				
proton	C110A	V68N′	V68D	V68E′	random coil
Leu29Cδ	−0.29	−0.33	−0.30	−0.30	0.94, 0.90
Leu29Cδ	−0.71	−0.69	−0.73	−0.69	0.94, 0.90
Phe43Cδ	7.32	7.28	7.22	7.32	7.30
Phe43Cε	6.13	6.12	6.12	6.16	7.39
Phe43Cζ	4.81	4.62	4.65	4.71	7.34
His64Cε	7.49	7.82	6.44	7.74	8.12
His64Cδ	4.84		5.94		7.14
Thr67Cγ	1.48	1.44	1.45	1.43	1.23
Ala71Cβ	2.48	2.54	2.52	2.55	1.39
Leu89Cγ		0.54	0.56	0.63	1.64
Leu89Cδ	0.38	0.26	0.34	0.33	0.94, 0.90
Leu89Cδ	0.77	0.74	0.72	0.78	0.94, 0.90
His93Cε	1.67	1.54	1.59	1.52	8.12
His97Cε	7.91	7.92	7.89	7.90	7.14
Met131Cε	2.28	2.28	2.28	2.27	2.13

[a] Also included for comparison are the random coil chemical shifts of these protons (Wüthrich, 1986).

suggest that the Asp in the former protein is ionized at pH 7.0. If the Asp were protonated, then one would expect the His64Cϵ proton in both of the above proteins to have a very similar chemical shift. Taken together with the isoelectric focusing and nondenaturing PAGE results, this suggests that, at pH 7.0, His64 forms a salt bridge with Asp68 in CO-V68D. Protonation of the His would ordinarily be expected to result only in downfield shifts for the Cδ and Cϵ protons relative to the unprotonated residue. However, His64 experiences large ring current shifts that are strongly position dependent. It is thus conceivable that the net effect of protonation coupled with changes in residue position could give rise to the observed shifts. The absence of changes in the chemical shift of the His64Cϵ proton in CO-V68E′ indicates that this residue remains unprotonated and hence that Glu68 is protonated in this protein.

Spectral Properties of ZnPChla–Mb Complexes. Incorporation of ZnPChl*a* into the heme pocket of apoMb is accompanied by characteristic changes in the CD spectrum of the chromophore (Wright & Boxer, 1981). These changes are caused by the slight distortion of the chromophore that is found to occur in the X-ray crystal structure of MgPChl*a*–SWMb (Lambright et al., unpublished results) or by coupled oscillator interactions of the chromophore with the $\pi\pi^*$ transitions of aromatic residues within the protein (Hsu & Woody, 1971). All mutant proteins reconstituted with ZnPChl*a* had very similar CD spectra (data not shown), indicating that the chromophore is binding in a similar orientation in the heme pocket in all cases.

The absorption spectrum of ZnPChl*a*–C110A is identical with that of ZnPChl*a*–SWMb (Wright & Boxer, 1981). Sample concentrations were estimated from the known value of 57 mM^{-1} cm^{-1} for the extinction coefficient of ZnPChl*a* in ZnPChl*a*–SWMb (Boxer & Wright, 1979). Absorption and fluorescence spectra were identical for all proteins except for ZnPChl*a*–V68D′. In this protein, the absorption maximum of the Q_y band is shifted from 661 to 666 nm, while the fluorescence maximum is shifted from 673 to 675 nm, corresponding to changes in energy of 114 and 44 cm^{-1}, respectively. Absorption spectra of ZnPChl*a* derivatives purified by isoelectric focusing confirmed that the spectral shift observed in ZnPChl*a*–V68D′ is not an artifact caused by the presence of aggregated protein.

All mutant proteins reconstituted with ZnPChl*a* had identical pfs (Figure 2, Table II), indicating that, as in the ZnPPIX derivatives, the carboxylate at either residue 68 or His64 (the distal His) is protonated in the ZnPChl*a* derivatives of V68D′ and V68E′. Note that ZnPChl*a* has one less carboxylate side chain than ZnPPIX, which accounts for the difference in the pfs of ZnPPIX- and ZnPChl*a*-reconstituted proteins and provides a convenient calibration of the effects of changing the charge on the pfs. NMR studies of the CO derivatives of these proteins described above suggest that the sites of protonation are Glu68 in ZnPChl*a*–V68E′ and His64 in ZnPChl*a*–V68D′. An Asp68–His64 salt bridge in ZnPChl*a*–V68D′ is also consistent with the fact that the absorption and fluorescence maxima of ZnPChl*a*–V68D′ are different from those of ZnPChl*a*–V68N′.

Estimation of the Apparent pK_a of Glu68 in ZnPChla–V68E′. The Q_y bands of ZnPChl*a*–C110A, ZnPChl*a*–V68N′, and ZnPChl*a*–V68D′ show no pH dependence in the pH range 5.5–9.5. Outside of this pH range there are either decreases in peak intensity or changes in peak position. These changes do not occur with well-defined isosbestic points and probably result from protein denaturation. The Q_y band of ZnPChl*a*–V68E′ is independent of pH in the range 5.0–7.5. However, at higher pH's, the Q_y band is red shifted with an isosbestic point at 665 nm (Figure 8). The absence of a pH dependence of the CD at 222 nm demonstrated that protein denaturation is insignificant at pH's below 9.3 (Varadarajan, 1988). The observed spectral shifts are probably due to ionization of Glu68. The apparent pK_a of the shifts was calculated by monitoring the absorbance at 673 nm as a function of pH and assuming that the spectral changes are due to ionization of a single residue within the protein. The following equation then describes the absorbance (A) at any wavelength within the Q_y band as a function of pH:

$$\mathrm{pH} = pK_a + \log\left[(A - A_p)/(A_d - A)\right] \qquad (4)$$

where A_p and A_d are the absorbances of the protonated and deprotonated forms of the protein. Since it is not possible to go to high enough pH to experimentally obtain A_d, both A_d and pK_a are obtained by a nonlinear least-squares fitting procedure using a Marquardt algorithm (Press et al., 1987). The average value of the apparent pK_a obtained from six separate determinations using several different preparations and concentrations of reconstituted protein was 8.87 ± 0.09.

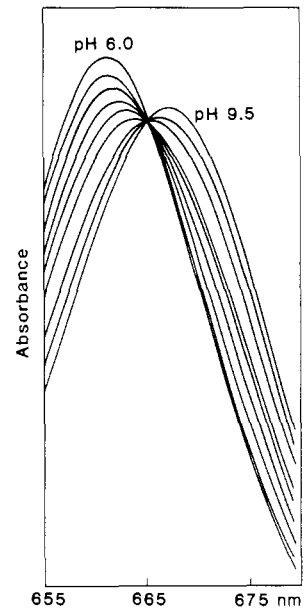

FIGURE 8: pH dependence of the Q_y absorption band of ZnPChl*a*–V68E′ in 10 mM sodium phosphate and 10 mM sodium borate, at 20 °C.

Because of protein denaturation at higher pH, it was not possible to determine the spectrum and hence the red shift of A_d. However, from observation of spectra at pH 9.6 (the highest pH at which the isosbestic point is preserved), it is unlikely that the shift is more than 6–7 nm. Thus, although spectral shifts relative to ZnPChl*a*–C110A are observed in ZnPChl*a*–V68E′ and ZnPChl*a*–V68D′, the shifts are much less than the values of about 25 nm (about 550 cm^{-1}) predicted to result from placement of a negative charge at a distance 3.5 Å from the plane of a chlorophyll *a* ring (Eccles & Honig, 1983). Involvement of Asp68 in a salt bridge with His64 would explain the small red shift observed in ZnPChl*a*–V68D′. In the case of ZnPChl*a*–V68E′ at high pH, the charge on the carboxylate is likely to be located close to the center of the porphyrin macrocycle. It may be that such a location is too far from the ring electron density to cause a large spectral shift. The calculations of Eccles and Honig were performed by assuming that the charged group and chlorin were interacting in vacuum (dielectric constant = 1). Buried charged groups in the interior of a protein must be stabilized, either by in-

Table V: pH Dependence of pK_{da}'s for Cyanide Binding to Mutant Mb's[a]

(A) pK_{da}'s in the pH Range 6.0–8.0

myoglobin	pH 6.0	pH 7.0	pH 8.0
C110A	4.89	5.72	6.58
V68D	3.52	3.42	3.53
V68E′	2.26	2.20	2.11

(B) Observed and Calculated pK_{da}'s in the pH Range 8.7–9.9

	pH 8.7		pH 9.0		pH 9.3		pH 9.6		pH 9.9	
myoglobin	obsd	calcd	obsd	calcd	obsd	calcd	obsd	calcd	obsd	calcd
V68D	3.36	3.45	3.30	3.41	3.09	3.24	2.92	3.09	2.71	2.86
V68E′	2.11	2.04	2.13	1.96	1.90	1.82	1.84	1.66	1.73	1.44

[a] The temperature of measurement was 28 ± 1 °C. The approximate errors in pK_{da}'s are ±0.1 on the basis of two to three separate determinations at pH 7.0.

teraction with other charged, dipolar and polarizable groups within the protein or by external solvent, as is clearly demonstrated by isoelectric focusing data on the heme- and ZnPPIX-containing mutant proteins. All such stabilizing interactions necessarily result in screening of the buried charge, making it unlikely that interactions between charged groups and nearby chromophores are the primary cause of the large red shifts observed in chlorophylls and bacteriochlorophylls associated with photosynthetic proteins. Similar arguments may explain results of recent studies of the spectral properties of site-specific mutants of bacteriorhodopsin (Mogi et al., 1988). Several Asp residues thought to be responsible for the red shift of the retinal chromophore were substituted by Asn, but none of these substitutions resulted in a substantial reduction of the observed red shift.

The free energy of transfer of a negatively charged residue from aqueous solution to the interior of a protein, $\Delta G°_{w\rightarrow p}$, is given by

$$\Delta G°_{w\rightarrow p} = 2.303RT(pK_{ap} - pK_{aw}) \quad (5)$$

where pK_{ap} and pK_{aw} are the pK_a's of the residue inside the protein and in aqueous solution, respectively (Warshel & Russell, 1985). The magnitude of $\Delta G°_{w\rightarrow p}$ provides information about the polarity of the protein interior. The pK_a of a glutamic acid residue exposed to aqueous solvent is 4.5 (Matthew, 1985). The shift of 4.4 pH units that appears to occur for Glu68 in ZnPChl*a*–V68E′ corresponds to a $\Delta G°_{w\rightarrow p}$ of 6.14 kcal/mol at 25 °C. Free energies of transfer from aqueous solution to water vapor have been measured for Glu, Asp, and several other amino acid side-chain analogues (Wolfenden et al., 1981). However, these measurements relate to transfer of the protonated, not the ionized, side chain and cannot be compared with the value of $\Delta G°_{w\rightarrow p}$ obtained above. If it is assumed that the carboxylate at residue 68 is completely solvent exposed in the denatured state of the protein, then $\Delta G°_{w\rightarrow p}$ is also an estimate of the electrostatic contribution to the destabilization caused by substituting Val68 by Glu in the ZnPChl*a*, ZnPPIX, deoxy, and CO derivatives of Mb.

Cyanide Binding. pK_{da}'s for cyanide binding at pH 7.0 for C110A, V68D, and V68E′ were determined to be 5.72, 3.42, and 2.20, respectively. The pK_{da} for V68N′ was at least 1 unit higher than for C110A and could not be accurately determined. Previously determined values of pK_{da} for SWMb range from 4.75 (Blanck et al., 1961) to 6.3 (Smith & McLendon, 1980). If CN^- binding at the heme iron is not accompanied by proton uptake by the protein, then the dissociation constant K_d is given by

$$K_d = [Mb][CN^-]/[MbCN] = K_{da}[CN^-]/[CN] \quad (6)$$

$$pK_d = pK_{da} - \log([CN^-]/[CN]) \quad (7)$$

HCN has a pK_a of 9.3 at 25 °C (Gordon & Ford, 1972). At pH's of 8.3 or below, $[CN^-]/[CN]$ would be expected to increase by about a factor of 10 per unit increase in pH. By assuming that the changes in the protein charge distribution that occur with pH do not affect pK_d significantly, pK_{da} would be expected to increase by approximately 1 unit per unit increase in pH. If cyanide binding is accompanied by proton uptake, then pK_d is given by

$$pK_d = pK_{da} - \log([HCN]/[CN]) \quad (8)$$

and at pH's below 8.3, pK_{da} should be essentially independent of pH. Apparent dissociation constants were therefore measured at pH 6.0, 7.0, and 8.0 (Table VA). The values in Table VA are clearly consistent with no proton uptake for C110A and with proton uptake for V68D and V68E′. This is consistent with the suggestion that the negatively charged carboxylates in the metaquo derivatives of V68D and V68E′ are stabilized by a favorable Coulombic interaction with the ferric heme iron. The loss of this interaction upon cyanide anion binding results in proton uptake by the protein and also increases the cyanide dissociation constant relative to C110A and V68N′. Unfavorable steric interactions between Glu68 and either bound cyanide or other nearby protein residues are also probable causes for the low cyanide binding affinity of V68E′.

In order to determine whether proton uptake upon cyanide binding in V68D and V68E′ also occurs at higher pH's, cyanide pK_{da}'s were measured at a series of pH's between 8.7 and 9.9 (Table VB). Also listed in Table VB are calculated pK_{da}'s assuming that cyanide binding is accompanied by proton uptake, the measured pK_{da}'s at pH 8.0 and the known pK_a value of 9.3 for HCN being used. Calculated pK_{da}'s for V68D are always found to be slightly larger than the observed values. This is reasonable because at higher pH's the protein becomes more negatively charged, resulting in a decrease in the observed pK_d and pK_{da}. For V68E′, calculated pK_{da}'s are always less than the observed ones. The reason for this is not obvious, but it may be indicative of ionization of Glu68 at high pH, as was suggested in the previous section.

Results of cyanide binding studies are also consistent with measurements of the reduction potential ($E°'$) of the heme iron in wild-type and mutant proteins (Varadarajan et al., 1989). We have observed large (approximately 200 mV) decreases in $E°'$ for V68D and V68E, relative to those of wild type and C110A. In the former two proteins, as with cyanide binding, reduction of the heme iron has been shown to be accompanied by proton uptake by the protein.

Since both reduction and cyanide binding are accompanied by proton uptake, it is not possible to use the changes in K_{da} and $E°'$ in V68D and V68E to estimate the magnitude of the electrostatic interaction between the carboxylate at residue 68 and the heme iron. As discussed above, the shift in the pK_a (ΔpK_a) of the residues involved in proton uptake, relative to

corresponding values in aqueous solution, provides information about the polarity of the protein interior. The free energy of folding (ΔG_{fold}) of Mb is approximately 10 kcal/mol (Pace & Vanderburg, 1979; Hughson & Baldwin, 1989). Although we have not yet experimentally determined ΔpK_a's of the residues involved in proton uptake, the fact that cyanide binding and reduction in V68D and V68E are not accompanied by protein unfolding puts an upper limit of about 7.3 units on this quantity since $\Delta pK_a \leq \Delta G_{fold}/2.303RT$.

Conclusions

These studies demonstrate that Mb is able to tolerate substitution of the buried hydrophobic residue Val68 by the polar residue Asn and the potentially charged residues Glu and Asp. Wild-type and all mutant proteins appear to be structurally very similar, with differences being localized mainly to residues 64 and 68. In the metaquo derivatives of V68E and V68D the pK_a's of the Glu and Asp substituents do not appear to be significantly shifted from their values in aqueous solution. The negative charge at residue 68 in these two proteins is stabilized by a favorable Coulombic interaction with the positively charged heme iron. In the metcyano, CO, deoxy, and ZnPCh*la* derivatives, the relatively nonpolar protein interior cannot solvate an isolated buried negative charge. At pH 7.0, the carboxylate at residue 68 is either protonated, as in CO-V68E, or stabilized via a salt bridge with the nearby residue His64, as in CO-V68D.

Absorption and fluorescence spectra of V68E′ and V68D′ reconstituted with ZnPCh*la* are similar to those of ZnPCh*la*–C110A. These results do not support the hypothesis that electrostatic interactions of nearby charged amino acid residues with the chromophore are the primary cause of the large red shifts observed in chlorophylls and bacteriochlorophylls associated with photosynthetic proteins. The apparent pK_a of Glu68 in ZnPCh*la*–V68E′ was estimated to be 8.9. The observed shift of 4.4 pK_a units from the value for Glu in aqueous solution provides a measure of the polarity of the protein interior.

There are large changes in the cyanide binding affinity and redox potential of the heme iron in the mutant proteins. In V68E and V68D both reduction and cyanide binding are accompanied by proton uptake by the protein. We hope that these results will stimulate theoretical calculations of the observed changes in redox thermodynamics and cyanide binding affinities and estimation of the pK_a's of the residues involved in proton uptake.

Acknowledgments

We thank S. Balasubramanian for purifying and characterizing C110A and Drs. J. R. Williamson, F. Hughson, and R. L. Baldwin for helpful discussions.

Registry No. Val, 72-18-4; Asn, 70-47-3; Asp, 56-84-8; Glu, 56-86-0; ZnPCh*la*, 41536-35-0; ZnPPIX, 15442-64-5; HEME, 14875-96-8; CN, 57-12-5; Fe, 7439-89-6.

References

Antonini, E., & Brunori, M. (1971) in *Hemoglobin and Myoglobin in Their Reactions with Ligands*, North-Holland, Amsterdam.

Blanck, J., Graf, W., & Scheler, W. (1961) *Acta Biol. Med. Germ. 7*, 323.

Boxer, S. G., & Wright, K. A. (1979) *J. Am. Chem. Soc. 101*, 6791–6794.

Bucks, R. R. (1981) Ph.D. Thesis, Stanford University.

Cooke, R. M., & Wright, P. E. (1985) *Biochim. Biophys. Acta 832*, 365–372.

Dalvit, C., & Wright, P. E. (1987) *J. Mol. Biol. 194*, 313–327.

Dickerson, R. E., & Geiss, I. (1983) *Hemoglobin*, Benjamin/Cummings, Menlo Park, CA.

Eccles, J., & Honig, B. (1983) *Proc. Natl. Acad. Sci. U.S.A. 80*, 4959–4962.

George, P., & Hanania, G. I. H. (1952) *Biochem. J. 52*, 517.

Gilson, M. K., & Honig, B. (1988) *Proteins, 3*, 32–52.

Gilson, M. K., Rashin, A., Fine, R., & Honig, B. (1985) *J. Mol. Biol. 183*, 503–516.

Gordon, A. J., & Ford, R. A. (1972) *The Chemist's Companion*, p 58, Wiley, New York.

Honig, B., Greenberg, A. D., Dinur, U., & Ebrey, T. G. (1976) *Biochemistry 15*, 4593–4599.

Hsu, M., & Woody, R. W. (1971) *J. Am. Chem. Soc. 93*, 3515–3525.

Hughson, F., & Baldwin, R. L. (1989) *Biochemistry* (in press).

Jue, T., & La Mar, G. N. (1984) *Biochem. Biophys. Res. Commun. 119*, 640–645.

Kolthoff, I. M., Sandell, E. B., Meehan, E. J., & Bruckenstein, S. (1969) *Quantitative Chemical Analysis*, p 741, Macmillan, London.

Kunkel, T. A. (1985) *Proc. Natl. Acad. Sci. U.S.A. 82*, 488–492.

Laemmli, U. K. (1970) *Nature (London) 227*, 680–685.

La Mar, G. N., Budd, D. L., Viscio, D. B., Smith, K. M., & Langry, K. C. (1978) *Proc. Natl. Acad. Sci. U.S.A. 76*, 5755–5759.

Lee, B., & Richards, F. M. (1971) *J. Mol. Biol. 55*, 379–400.

Mabbutt, B. C., & Wright, P. E. (1985) *Biochim. Biophys. Acta 832*, 175–185.

Makinen, M. W., & Churg, A. K. (1983) in *Iron Porphyrins* (Lever, A. B. P., & Gray, H. B., Eds.) Part 1, p 141, Addison-Wesley, Reading, MA.

Marion, D., & Wüthrich, K. (1983) *Biochem. Biophys. Res. Commun. 113*, 962–974.

Marston, F. A. O., Lowe, P. A., Doel, M. T., Schoemaker, J. M., White, S., & Angal, S. (1984) *Bio/Technology 2*, 800–804.

Matthew, J. B. (1985) *Annu. Rev. Biophys. Biophys. Chem. 14*, 387–417.

McClellan, T. (1984) *Biochem. Genet. 22*, 181–200.

Messing, J. (1983) *Methods Enzymol. 101*, 21–98.

Mogi, T., Stern, L. J., Marti, T., Chao, B. H., & Khorana, H. G. (1988) *Proc. Natl. Acad. Sci. U.S.A. 85*, 4148–4152.

Moore, G. R., Leitch, F. A., Pettigrew, G. W., Rogers, N. K., & Williams, G. (1986) in *Fronteirs in Bioinorganic Chemistry* (Xavier, A. V., Ed.) p 494, VCH, Weinheim, Federal Republic of Germany.

Nagai, K., & Thogersen, H. C. (1984) *Nature (London) 309*, 810–812.

Pace, N. C., & Vanderburg, K. E. (1979) *Biochemistry 18*, 288–292.

Perutz, M. F., Pulsinelli, P. D., & Ranney, H. M. (1972) *Nature (London) New Biol. 237*, 259–264.

Press, W. H., Flannery, B. P., Teukolsky, S. A., & Wetterling, W. T. (1987) *Numerical Recipes*, pp 498–539, Cambridge University Press, Cambridge, U.K.

Rance, M., Sorensen, O. W., Bodenhausen, G., Wagner, G., Ernst, R. R., & Wüthrich, K. (1983) *Biochem. Biophys. Res. Commun. 117*, 479–485.

Rees, D. C. (1980) *J. Mol. Biol. 141*, 323–326.

Russell, A. J., & Fersht, A. R. (1987) *Nature (London) 328*, 496–500.

Sanger, F. (1981) *Science 214*, 1205–1210.
Scouloudi, H., & Baker, E. N. (1978) *J. Mol. Biol. 126*, 637–660.
Shulman, R. G., Wüthrich, K., Yamane, T., Patel, D. J., & Blumberg, W. E. (1970) *J. Mol. Biol. 53*, 143–157.
Smith, M. C., & McLendon, G. (1980) *J. Am. Chem. Soc. 102*, 5666–5670.
States, D. J., Haberkorn, R. A., & Ruben, D. J. (1982) *J. Magn. Reson. 48*, 286–292.
Steadman, J. H., Yates, A., & Huehns, E. R. (1970) *Br. J. Haematol. 18*, 435–446.
Takano, T. (1977) *J. Mol. Biol. 110*, 537–568.
Teale, F. W. J. (1959) *Biochim. Biophys. Acta 35*, 543.
Varadarajan, R. (1988) Ph.D. Thesis, Stanford University.
Varadarajan, R., Szabo, A., & Boxer, S. G. (1985) *Proc. Natl. Acad. Sci. U.S.A. 82*, 5681–5684.
Varadarajan, R., Zewert, T. E., Gray, H. B., & Boxer, S. G. (1989) *Science 243*, 69–72.
Warshel, A., & Russell, S. T. (1985) *Q. Rev. Biophys. 17*, 283–422.
Warwicker, J., & Watson, H. C. (1982) *J. Mol. Biol. 157*, 671–679.
Wolfenden, R., Anderson, L., Cullis, P. M., & Southgate, C. C. B. (1981) *Biochemistry 20*, 849–855.
Wright, K. A., & Boxer, S. G. (1981) *Biochemistry 20*, 7546–7556.
Wüthrich, K. (1986) *NMR of Proteins and Nucleic Acids*, p 17, Wiley, New York.

Amino Acid Sequences of Pyridoxal 5′-Phosphate Binding Sites and Fluorescence Resonance Energy Transfer in Chicken Liver Fatty Acid Synthase†

Soo-Ik Chang and Gordon G. Hammes*
Department of Chemistry, Cornell University, Ithaca, New York 14853-1301
Received November 29, 1988; Revised Manuscript Received January 13, 1989

ABSTRACT: The amino acid sequences associated with pyridoxal 5′-phosphate binding sites in chicken liver fatty acid synthase have been determined: a site whose modification causes selective inhibition of the enoyl reductase activity and a site (site I) that is not associated with enzymatic activity. The amino acid sequences of peptides obtained by trypsin hydrolysis of the pyridoxamine 5′-phosphate labeled enzyme were determined. For the site associated with enoyl reductase activity, the sequence similarities between chicken and goose are extensive and include the sequence Ser-X-X-Lys, a characteristic structural feature of pyridoxamine enzymes. In addition, the spatial relationships between the pyridoxal 5′-phosphate binding sites and reductase site(s) have been studied with fluorescence resonance energy-transfer techniques. The distances between site I and the enoyl reductase and β-ketoacyl reductase sites are >50 and 41–44 Å, respectively. The distance between the two reductase sites is >49 Å.

Fatty acid biosynthesis is one of the most important processes in living organisms. It is essential for the growth of cellular membranes. The fatty acid synthase enzyme catalyzes fatty acid synthesis according to

$$\text{acetyl-CoA} + n\text{malonyl-CoA} + 2n\text{NADPH} + 2n\text{H}^+ \rightarrow \text{CH}_3(\text{CH}_2\text{CH}_2)_n\text{COR} + (n+1)\text{CoA} + n\text{CO}_2 + 2n\text{NADP}^+ + (n-1)\text{H}_2\text{O}$$

where R is OH or CoA.[1] Animal fatty acid synthase has three essential substrate-binding sites: serine, a substrate "loading" site; 4′-phosphopantetheine, a substrate "carrier" site; and cysteine, a substrate "waiting" site (Nixon et al., 1970; Wakil et al., 1983; Chang & Hammes, 1988). To synthesize palmitic acid or palmityl-CoA ($n = 7$), the enzyme carries out 37 sequential reactions. The organization of fatty acid synthase varies from species to species. In most procaryotes, fatty acid synthesis is carried out by seven separable monofunctional enzymes and acyl-carrier protein [cf. Volpe and Vagelos (1973)]. However, in eucaryotes, a multienzyme complex is utilized (Wood et al., 1978; Wakil et al., 1983; Schweizer, 1986). The evolutionary aspects of fatty acid synthase have been extensively discussed (Poulose et al., 1981; Hardie & McCarthy, 1986; Witkowski et al., 1987; Chang & Hammes, 1988).

The structure of chicken liver fatty acid synthase ($M_r \sim 500\,000$) has been probed by limited proteolysis and chemical modification [cf. Wakil et al. (1983)]. The two identical polypeptides are arranged head-to-tail with two independent catalytic centers, each derived from two different polypeptide chains. A structural model for the enzyme has been constructed from small-angle neutron-scattering and electron microscope studies (Stoops et al., 1987). The polypeptides have dimensions of 160 × 146 × 73 Å, with three domains having lengths of 32, 82, and 46 Å. Limited tryptic digestion yields three protein bands on sodium dodecyl sulfate–polyacrylamide gels (Tsukamoto et al., 1983). Domain I ($M_r \sim 127\,000$), the N-terminal region of the protein, contains the acyl transferases and β-ketoacyl synthase. Domain II ($M_r \sim 107\,000$) contains the dehydratase, enoyl reductase, β-ketoacyl reductase, and the acyl-carrier protein. Domain III ($M_r \sim 33\,000$), the C-terminal region, is the thioesterase.

† This work was supported by a grant from the National Institutes of Health (GM 13292).

[1] Abbreviations: CoA, coenzyme A; NADPH, reduced nicotinamide adenine dinucleotide phosphate; HPLC, high-performance liquid chromatography; EDTA, ethylenediaminetetraacetic acid; Tris, tris(hydroxymethyl)aminomethane; TNADPH, reduced thionicotinamide adenine dinucleotide phosphate; TPCK, L-1-(tosylamino)-2-phenylethyl chloromethyl ketone.

0006-2960/89/0428-3781$01.50/0 © 1989 American Chemical Society